AGU PUBLICATIONS

Paleoceanography

RESEARCH ARTICLE
10.1002/2014PA002615

Key Points:
- Miocene
- Accuracy of the orbitally tuned time scale
- Milankovitch theory

Supporting Information:
- Readme
- Table S1
- Table S2
- Text S1
- Figure S1
- Figure S2
- Figure S3

Correspondence to:
C. Zeeden,
c.zeeden@geo.rwth-aachen.de

Citation:
Zeeden, C., F. J. Hilgen, S. K. Hüsing, and L. L. Lourens (2014), The Miocene astronomical time scale 9–12 Ma: New constraints on tidal dissipation and their implications for paleoclimatic investigations, *Paleoceanography*, *29*, 296–307, doi:10.1002/2014PA002615.

Received 21 JAN 2014
Accepted 17 MAR 2014
Accepted article online 23 MAR 2014
Published online 17 APR 2014

The Miocene astronomical time scale 9–12 Ma: New constraints on tidal dissipation and their implications for paleoclimatic investigations

Christian Zeeden[1,2], Frederik J. Hilgen[1], Silja K. Hüsing[3], and Lucas L. Lourens[1]

[1]Faculty of Geosciences, University of Utrecht, Utrecht, Netherlands, [2]Now at Chair of Physical Geography and Geoecology, RWTH Aachen University, Aachen, Germany, [3]Paleomagnetic Laboratory 'Fort Hoofddijk', Faculty of Geosciences, Utrecht University, Utrecht, Netherlands

Abstract Orbital tuning and understanding climate response to astronomical forcing in the Miocene require detailed knowledge of the effect of tidal dissipation (Td) and dynamical ellipticity (dE) on astronomical solutions used to compute insolation and orbital target curves for paleoclimatic studies. These Earth parameters affect precession and obliquity; the determination of their effect is of fundamental importance, as phase relations between astronomical forcing and climate response can only be accurately calculated when the relative phasing between precession and obliquity is known. This determination can be achieved through comparison of solutions having different values for Td and/or dE with well-understood paleoclimate data. In this paper we use quantitative color records of precession-obliquity interference recorded in two successive 2.4 Myr eccentricity minima (9–9.6 and 11.5–12.1 Ma) in the Monte dei Corvi section in northern Italy to constrain the effect of Td, using the assumption of a direct response of sapropels to insolation. This quantitative approach results in a minimum uncertainty of astronomically tuned age models of ± 0.8 kyr and Td values 0.95 and 1.05 for the 9–9.6 Ma interval and of +4/−1 kyr (Td values between 0.95 and 1.15) for the 11.5–12.1 Ma interval. This (un)certainty not only limits the precision of determining phase relations but also improves our understanding of the limitations of tuned time scales and determining phase relations in the Miocene.

1. Introduction

The determination of the phase relation between astronomical forcing, i.e., insolation, and Earth's climate response recorded in paleoclimate archives is of major interest in paleoclimatology. For the Pleistocene, this is usually achieved by a combination of different dating methods, including radioisotopic dating (^{14}C, U/Th, and Ar/Ar) and astronomical tuning. Most important for our study, *Ziegler et al*. [2010] demonstrated the consistency of astronomical ages for Mediterranean sapropels (time delayed in the late Pleistocene due to north Atlantic cold events) with U/Th dated speleothems.

High-resolution time scales in older time intervals often rely on orbital tuning supported by magnetobiostratigraphy, $^{40}Ar/^{39}Ar$ and/or $^{238}U/^{206}Pb$ dating, but often lack the necessary confirmation or intercalibration from independent radioisotopic studies. In addition, a reliable intercalibration of these methods is required for consistency and incorporation in the standard Geological Time Scale [*Kuiper et al*. 2008; *Rivera et al*., 2011]. Here uncertainties in the precession and obliquity frequencies that result from (possibly) changing values of tidal dissipation (Td) and dynamical ellipticity (dE) in the astronomical solution start to play a critical role. The effect of Td on precession and obliquity is almost negligible for young time intervals, i.e., the late Pleistocene, but increases rapidly and nonlinearly back in time [see *Lourens et al*., 2004, Figure 21.7]. Consequently, for older time intervals such as the Miocene, it is essential to constrain the effect of Td and dE in order to improve our understanding of the response time of Earth's climate system to orbital forcing and also to obtain a tuned time scale with highest accuracy and precision. These values, which are denoted between brackets in subscript behind the astronomical solution (e.g., $La2004_{(dE,Td)}$, where (1,1) represents the present-day values for dynamical ellipticity and tidal dissipation and higher/lower values represent increased/decreased average values of Td or dE over the considered time interval), cannot be directly verified by astronomical theory but have to come from a detailed comparison with paleoclimate data.

Td and the associated change in precession and obliquity frequencies is parameterized relative to the recent rate of change in the motion of the Moon [*Laskar et al*., 1993]; it is considered constant over the time interval analyzed in the *Quinn et al*. [1991], *Laskar* [2001], and the *Laskar et al*. [1993, 2004] algorithms. *Laskar et al*. [2004] defined the dynamical ellipticity as Ed = (2C − A − B)/C, where A, B, and C are the principal axis of inertia with A < B < C. Again, dE is parameterized relative to the recent value by *Laskar et al*. [1993, 2004]. The La90, 93, La2001, and La2004 solutions [*Laskar*, 1990; *Laskar et al*., 1993; *Laskar*, 2001; *Laskar et al*., 2004] are analytical solutions, numerically integrating information of all eight planets. Improving on the previous solutions, the La2004 solution uses a direct integration of the gravitational equations for the orbital motion and improves the dissipative contributions, in particular in the evolution of the Earth-Moon System. Further, the La2004 uses more precise initial conditions [*Laskar et al*., 2004]. Both Td and dE are considered in the calculation of the precession constant and therefore have a direct effect on precession and obliquity frequencies. The issue of potentially variable Td and dE values has been investigated in sedimentary geoarchives before by *L. Lourens et al*. [1996, 2001] and *Pälike and Shackleton* [2000]. Using the Ti/Al elemental ratio in deep-sea sediments from Ocean Drilling Program (ODP) Site 967 as proxy for relative aridity, *Lourens et al*. [2001] demonstrated that the present-day values for Td and dE in the La90 solution [*Laskar*, 1990] resulted in a good match with the precession-obliquity interference patterns in the paleoclimatic record for the interval between 2.4 and 2.9 Ma. However, the La90 solution with a Td parameter of 0.5 (thus an in-average halved Td over the last 2.9 Ma) gives even more consistent results with the geological record, though these options are statistically indistinguishable [*Lourens et al*., 2001]. This is in agreement with results of a visual comparison of older cycle patterns in land-based marine sections [*L. Lourens et al*., 1996]. Keeping dE constant at its present-day value, the results of *Lourens et al*. [2001] suggest a Td <1. *Lourens et al*. [2001] did not compute uncertainties for their results but considered "an infinity of solutions ranging between La90(1.0003,0) and La90(0.9997,1)" to give results consistent with the geological sapropel record; the very similar correlation coefficient values seem statistically indistinguishable for solutions with the present-day and different Td values, also because differences between solutions are still very small in this relatively young interval [see *Lourens et al*., 2001, Figures 3 and 4; see also *Lourens et al*., 2004].

Pälike and Shackleton [2000] used high-resolution proxy records from ODP Site 926 (Ceara Rise, western equatorial Atlantic) to quantify the average values of Td and dE between 0 and 11.5 Ma, and between 17.5 and 24 Ma in the La1993 solution [*Laskar et al*., 1993]. They concluded, in agreement with *Lourens et al*. [2001], that average values for Td and dE cannot be distinguished from the present-day values (1). Recently, *Zeeden et al*. [2013] published a revised splice for ODP Site 926, mainly because the precession amplitudes presented by *Shackleton and Crowhurst* [1997] showed some major inconsistencies with eccentricity. *Zeeden et al*. [2013] used newly generated high-resolution physical property data (color and magnetic susceptibility) to demonstrate that the original shipboard splice used by *Pälike and Shackleton* [2000] is incorrect in parts, in particular for the interval between 10 and 13.6 Ma. Note that *Shackleton and Crowhurst* [1997] already suggested that higher resolution physical property data might improve the original age model. This resulted in a different tuning; as a consequence, estimations of Td and dE by *Pälike and Shackleton* [2000] may be less accurate for this interval.

Morrow et al. [2012] discuss that the consistently relatively small change in Td and/or dE over the last ~3 and ~25 Myr presented by *Lourens et al*. [2001] and *Pälike and Shackleton* [2000] are inconsistent with the assumption of dynamical ellipticity being dominated by the effects of ice ages over the last ~3 Ma and by mantle convection over longer time scales, i.e., 25 Ma. Furthermore, *Morrow et al*. [2012] suggest that time scale-dependent mantle behavior, the combined effect of Td and dE, an unrealistically narrow bound of dE by geological data, or Earth models with opposite and about canceling effects of ice loading and mantle convection may resolve the apparent enigma. However, modeling results seem so far inconsistent with geological observations. No claim is made in this study about values for Td and dE, because these parameters can have the same effect on orbital cycle patterns.

Here we investigate the combined effect of Td and dE on the geological timescale. Quantitative color records of intricate cycle patterns related to precession-obliquity interference in the deep marine sapropel-bearing succession of the Monte dei Corvi section are used in this study to investigate the combined effect of Td and dE in Miocene times. A visual comparison suggested that different Td values may have to be applied (keeping dE fixed at its present-day value) for different time intervals to get the best possible qualitative fit with the astronomical solution [*Hilgen et al*., 2003; *Hüsing et al*., 2007], but a quantitative study has not yet been undertaken. The advantage of this record is that an in-phase relation between insolation forcing (and thus forcing by precession, obliquity, and eccentricity) and climate response can be assumed for both the precession and obliquity signal (analogous to *Lourens et al*. [2001]), as both have been shown to relate to the African monsoon and thus likely share the same climatic origin [*Tuenter et al*., 2003]. This important assumption of a direct response, in the absence of marked glacials, is supported by transient climate modeling experiments [*Weber and Tuenter*, 2011].

2. Geological Setting and Section

The Miocene cyclic deep marine succession exposed in the coastal cliffs south of Ancona in Italy has been intensively studied. In particular, it has been used to establish an integrated stratigraphy and tuned time scale for the interval between ~6.1 and ~16.2 Ma [*Cleaveland et al*., 2002; *Hilgen et al*., 2003; *Hüsing et al*., 2007, 2009a, 2009b, 2010; *Mader et al*., 2001, 2004; *Montanari et al*., 1997; *Mourik et al*., 2010; *Turco et al*., 2011]. The Tortonian Global Stratotype Section and Point is defined in this section [*Hilgen et al*., 2005], and the astronomically tuned ages for reversal boundaries from the interval between 14.9 Ma and 8.7 Ma have been incorporated in the standard geological time scale for the Neogene [*Hilgen et al*., 2012 in *Gradstein et al*., 2012]. The sedimentary cycles have been related to astronomical climate forcing using their lithological expression that changes throughout the succession [*Hilgen et al*., 2003; *Hüsing et al*., 2007, 2010; *Montanari et al*., 1997; *Mourik et al*., 2010].

The basic cycle consists of a gray marl and whitish limestone. Between ~9.5 and ~13.6 Ma, brownish to blackish organic-rich beds, commonly referred to as sapropels, are frequently intercalated in the limestone beds of the cycles, resulting in a quadruplet buildup (see *Hilgen et al*. [2003, Figure 2] for an illustration). In the interval younger than ~9.5 Ma, the basic cycle represents a couplet of a gray marl and sapropel. In the older part (11.5–12.3 Ma), the quadruplet buildup of the basic cycle (marl-limestone[-sapropel-limestone]) has been linked to precession [*Hilgen et al*., 2003], whereby sapropels correspond to precession minima and summer insolation maxima (65°N latitude), i.e., the same phase relation as for younger sapropels in the Mediterranean [e.g., *Hilgen*, 1991]. Small-scale and large-scale sapropel clusters relate to 100 kyr and 405 kyr eccentricity maxima, respectively. Alternating thick/thin and/or distinct/vague sapropels have been related to precession/obliquity interference [*Hilgen et al*., 2003].

For this study, two intervals between 9 and 9.6 Ma, and 11.5 and 12.1 Ma were selected in the Monte dei Corvi section. These intervals represent successive minima in the 2.4 Myr eccentricity cycle. During such eccentricity minima, the amplitude and geological expression of the ~100 kyr cycle is reduced due to destructive interference ("canceling-out") of individual precession components (see also supporting information Figure S1). This results in low-amplitude variations in precession and a relative increase in obliquity, resulting in intricate precession-obliquity interference patterns over a prolonged interval of time (see Figure S1 for an example). These precession-obliquity interference patterns, where sapropels are linked to precession minima and obliquity maxima, are the subject of investigation here; we assume a direct response of sapropels to precession and obliquity-related changes in summer insolation.

3. Methods

Color measurements were performed with a Minolta CM-600d photo spectrometer at a 3–5 cm resolution in the two intervals, resulting in an average temporal resolution of about 1–1.4 kyr. Measurements were made at the foot of the cliffs where outcrop conditions are most favorable. Where necessary, the surface was cleaned to expose unweathered sediment. To improve the quality of the data, three measurements were made per stratigraphic level, which were later averaged. The mean coefficient of variance of spectral color measurements is 0.16 for the 9–9.6 Ma interval and 0.044 for the 11.5–12.3 Ma interval. The quadruplet structure with a dark sapropel between light limestone beds in the interval between ~11.5 and 12.1 Ma prevents the direct application of the lightness or spectral color data as proxy. A new lithological color index (LCI) was therefore generated using principal component analysis of the spectral color data and combining the second principal component with the lightness data. Detailed description of the construction of this LCI is provided in the supporting information.

For comparison with the La201b10 solution [*Laskar*, 2001], the proxy records (lightness, L*, and LCI) from both intervals are tuned to a p-0.5 t target curve (normalized precession minus 0.5*normalized obliquity/tilt) [see *L. Lourens et al*., 1996]. As in *Lourens et al*. [2001], the geological data, orbital target, and tie points are dominated by precession, allowing the obliquity component to keep its original phase relative to different tuning targets.

For cross-spectral analysis, the Blackman-Tukey method [*Blackman and Tukey*, 1958] is used as implemented in the Analyseries software [*Paillard et al*., 1996]. Frequency bands that correspond to periods of 18–26 and

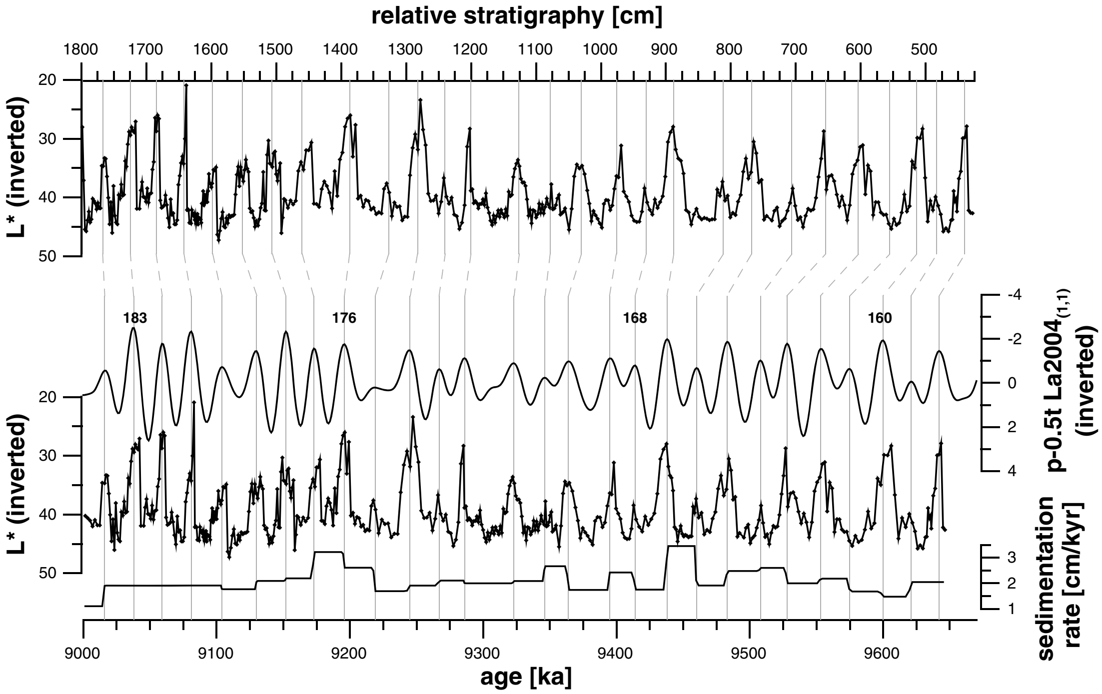

Figure 1. Tuning of the interval from ~9 to 9.65 Ma using the lightness (L*) data from Monte dei Corvi. Orbital tuning of the depth series to the $La2004_{(1,1)}$ p-0.5 t target follows *Hüsing et al.* [2007], their numbering of sapropels is included. Resulting sedimentation rates are plotted at the bottom.

38–46 kyr are investigated for the phase of precession and obliquity, respectively. Phases, and also minima/maxima at the 90% confidence level, are averaged over these frequency bands, i.e., the period ranges indicated just above. It is assumed that the obliquity phase is a reliable indicator for the consistency between solution and data. From the 11.5–12.1 Ma data set, it becomes clear that the obliquity phase is more sensitive to the Td variations than the correlation; therefore, we preferentially rely on the obliquity phase.

To evaluate the fit of a tuning using specific Td values with proxy data, the Spearman rank correlation coefficient [*Spearman*, 1904] is calculated between the tuned proxy data set and the tuning target. In contrast to the commonly used Pearson correlation coefficient [*Pearson*, 1896], the Spearman Rank correlation allows for some nonlinearity. To facilitate this, the orbital solution is interpolated at times of proxy data availability. The 90% confidence levels of the correlation coefficient are computed using 10,000 simulations using bootstrap resampling with replacement [*Efron and Gong*, 1983]; at least 75% of the original data were used for each resampling. The significance of correlations was calculated using 100,000 phase randomized surrogates (for each of the data sets) as described in *Ebisuzaki* [1997], using the *Meyers* [2014] code.

Values for Td were modified in the La2001b10 solution (J. Laskar, unpublished data, 2001), which allows adjustment of these parameters similar to the *Laskar et al.* [1993] routine. The La2001b10 and La2004 solutions are nearly identical over the last 15 Ma for recent values of Td and dE (1,1; see Figure S1 for the 11.5–12.1 Ma time interval); they are therefore interchangeable and can be directly compared for this interval. The Td parameter in La2001b10 is changed in steps of 0.1, while dE is kept constant. Only Td is changed as both parameters have the same effect on precession and obliquity, and no clear distinction between these two parameters can be made from geological records. The approach of *Lourens et al.* [2001] is applied; additionally, uncertainties in the squared Spearman rank correlation coefficient are included.

The data from this manuscript can be accessed at http://doi.pangaea.de/10.1594/PANGAEA.824094.

4. Results

The L* data in the interval from ~9 to 9.6 Ma show clear alterations of high and low values in a semiregular pattern (Figure 1). The L* minima correspond to the sapropels, and L* maxima to the lighter colored marls in between the sapropels. The data do not follow a sinusoidal curve but start in the older interval from a slightly

Table 1. Obliquity Phases and Correlation Coefficients (Squared Spearman Rank Correlation) for the Tunings Discussed Using Different Td Values[a]

Tuning to La2001b10 using a Td of 9–9.6 Ma	Precession Phase (18–25 kyr) in Degrees			Obliquity Phase (38–45 kyr)			Squared Spearman Rank Correlation	90% Confidence Correlation
	Average	Min	Max	Average	Min	Max		
1.2	−0.37	−7.25	6.51	−22.93	−32.86	−12.99	0.381	0.026
1.1	0.66	−6.36	7.69	−12.19	−21.59	−2.79	0.397	0.026
1	−2.37	−8.85	4.11	2.57	−8.75	13.88	0.391	0.027
0.9	−3.27	−10.49	3.95	12.83	3.08	22.59	0.384	0.027
0.8	−5.66	−12.36	1.05	24.17	13.94	34.40	0.374	0.027
0.7	−3.42	−10.52	3.67	37.10	26.32	47.87	0.358	0.027
0.6	−6.45	−13.47	0.58	49.89	39.25	60.52	0.336	0.027
0.5	−9.70	−16.67	−2.73	63.47	51.92	75.03	0.319	0.025
0.4	−8.12	−16.46	0.23	71.63	60.09	83.17	0.293	0.025
0.3	5.43	−2.14	12.99	−50.73	−60.88	−40.58	0.325	0.024
0.2	1.78	−5.78	9.34	−40.53	−51.04	−30.03	0.365	0.025
Tuning to La2001b10 using a Td of 11.5–12.3 Ma								
1.2	−8.40	−13.90	−2.90	−21.56	−34.47	−8.65	0.496	0.018
1.1	−7.00	−12.50	−1.51	−7.71	−21.29	5.87	0.490	0.019
1	−2.37	−8.84	4.09	1.31	−9.34	11.97	0.467	0.020
0.9	−9.56	−15.10	−4.01	17.15	2.89	31.41	0.457	0.020
0.8	−10.34	3.74	−5.05	33.33	17.53	49.13	0.426	0.021
0.7	−11.33	6.79	−6.19	50.26	34.02	66.51	0.406	0.020
0.6	−11.42	30.28	−7.05	66.40	48.51	84.30	0.373	0.020
0.5	−9.38	−15.01	−3.76	85.35	65.19	105.51	0.486	0.019
0.5	−5.27	28.36	−1.03	−29.00	−42.87	−15.13	0.333	0.019
0.4	−9.17	−15.76	−3.66	−10.23	−19.75	4.06	0.480	0.019
0.3	−9.81	−16.35	−4.25	−0.55	−40.76	−14.79	0.465	0.020
0.2	−10.07	−16.75	−4.82	14.06	0.09	28.03	0.448	0.020

[a]For the 11.5–12.1 Ma interval, two tunings were accomplished for Td = 0.5. The Td values in italic represent tunings shifted by one precession cycle relative to the tuning with Td = 0.6.

undulating baseline of low L* values (~45) from which distinct minima typically reach values of ~30. These minima are more closely spaced (~45 cm) in the younger part of the record (~1400–1800 cm) than in the older part, where the spacing of the distinct minima is approximately twice that of the younger part. Exceptions are successive peaks around 600 and 1000 cm, which are more closely spaced again. Less distinct L* minima are often found in between the more widely spaced minima of the older part and coincide with less distinct and thinner sapropels. The tuning of the 9–9.6 Ma interval to the $La2004_{(1,1)}$ solution is straightforward with the pattern of L* minima matching that of the p-0.5 t target curve (see also the tunings of *Hilgen et al.* [2003] and *Hüsing et al.* [2007]). The L* minima trace the precession-obliquity interference pattern in the target curve well and reveal the abrupt transition to a more precession-dominated pattern around 9.2 Ma. In particular, the precession-obliquity interference in L* between ~500 and ~1300 cm provides an excellent fit with the astronomical target curve, including the switch in the interference pattern around 9.55 Ma (Figure 1). In the geological record, one sapropel seems to be "missing"; here the relatively weak p-0.5 t peak is assumed to have been too weak for a sapropel formation. Further, some additional small-scale minima occur in the L* data set, which are not represented in the orbital solution (at ~9.19, ~9.3, and ~9.39 Ma). This may be caused by noise (e.g., due to a noisy record and bioturbation) or by a nonlinear recording of this record to orbital forcing. Tuning tie points are given in the supporting information Table S1.

For the ~9–9.6 Ma interval, the tuned L* record is compared with the p-0.5 t target curve for La2001b10 solutions with Td varying between 0.2 and 1.2 (in steps of 0.1). This comparison shows that an in-phase relationship with obliquity is accomplished for a Td value of 1 (see Figure 3 and Table 1). Correlation between L* and the target curve is significant at >99.9% confidence level for all correlations and is highest for a Td value of 1.1, but values of 1 and 0.9 are almost equally good and cannot be statistically distinguished at the 90% confidence level. The La2001b10 solution with Td values deviating from 1 results in obliquity phases inconsistent with the assumption of a direct climate response to insolation for sapropels (at 90% confidence

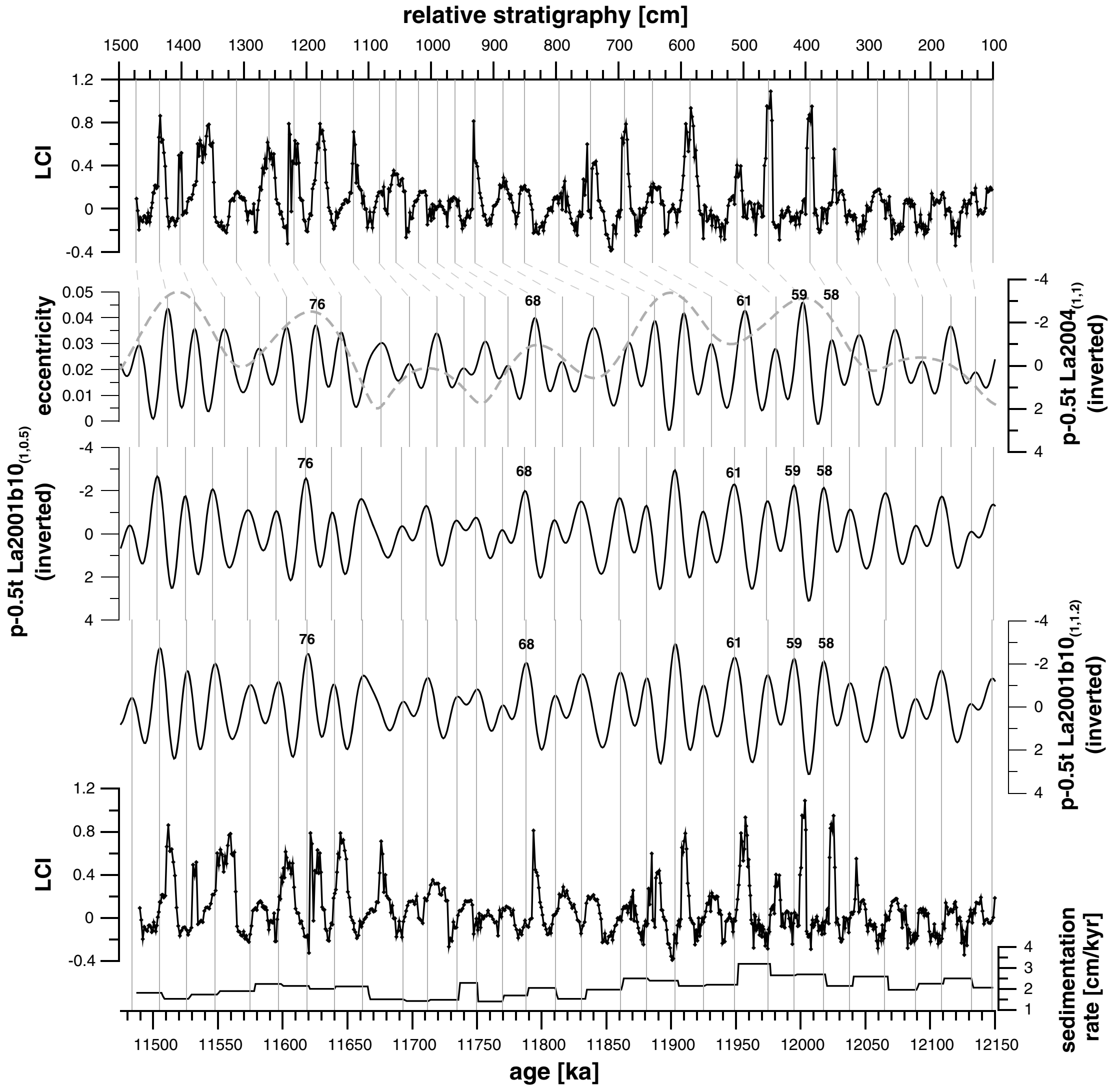

Figure 2. Tuning of the interval from ~11.5 to 12.15 Ma using the lithological color index (LCI) as generated from color data from the Monte dei Corvi outcrop. Also see the caption of Figure 1 and the text for further explanations.

level) and, hence, no in-phase relation with obliquity. For Td values of 0.3 and 0.2, the tuning had to be shifted one precession cycle to obtain a decent fit between geological data and the orbital solution.

The interpretation of the color data is less straightforward for the older interval (11.5–12.1 Ma, Figure 2) because of the quadruplet structure of the basic cycles, and the dark sapropels occurring between the relatively light limestones (sapropel-limestone-marl-limestone alterations) [see *Hilgen et al.*, 2003, Figure 2]. Our description and interpretation thus starts from the LCI (see supporting information) record directly; maxima in the LCI from ~11.5 to 12.1 Ma correspond to sapropels, minima to the gray marls. An antiphase relationship between p-0.5 t and the L* (Figure 2) therefore exists. These minima reach baseline values of approximately −0.2. The maxima that appear from this baseline reveal a clear pattern; in the younger part (1100–1500 cm), two groups of three and four distinct LCI maxima can be distinguished with one weak maximum in between (at 1315 cm). These groups define two successive small-scale sapropel bundles that reflect ~100 kyr eccentricity maxima (Figure 2, following the tuning of *Hilgen et al.* [2003] and *Hüsing et al.* [2007]). No obvious clustering of LCI maxima is observed in the older part. Here distinct maxima are only found between 400 and 750 cm, except for a single maximum at 920 cm. These maxima correspond to prominent and thicker sapropels. They reveal an alternation of distinct and less distinct maxima between 450 and 700 cm that represents precession-obliquity interference as also reflected in the sapropels (following the interpretation of *Hilgen et al.* [2003]). The tuning of this older

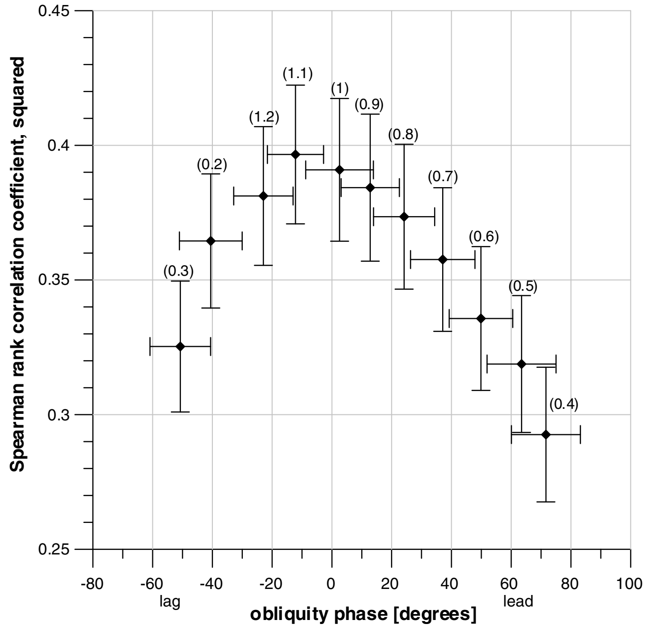

Figure 3. Plot of the squared Spearman rank correlation coefficient (ordinate) versus the obliquity phase (abscissa) of all investigated tunings for the interval from 9 to 9.6 Ma. The Td value used for every data point is included. For low Td values (0.2, 0.3), the tuning was shifted by one precession cycle.

interval, which follows that of *Hilgen et al*. [2003] and *Hüsing et al*. [2007], is less straightforward as no perfect visual match is found with the target curve of a particular solution. For instance, the two prominent LCI maxima at 395 and 465 cm are better reflected in the p-0.5 t target curve of the La2001b10$_{(1,0.5)}$ and La2001b10$_{(1,1.2)}$ solutions than in La2001b10$_{(1,1)}$. However, the two successive prominent maxima at ~690 and 750 cm are better mirrored in the target curve of La2004$_{(1,1)}$. The fact that no excellent fit of the Monte dei Corvi data and the orbital solution is found may originate from the fact that the Td is assumed to be constant over the entire time interval discussed, which is probably not the case. Also, the assumption of a direct response to climate forcing for sapropels, or a combination of both reasons, may explain the observed misfit. Tuning tie points are given in the supporting information Table S2.

Because maxima in the LCI correspond to sapropels and thus show an antiphase relationship with p-0.5 t, or the L* (Figure 2), obliquity phases are shifted by 180° (π) for direct comparison with the younger interval. Cross-spectral analysis of the tuned LCI record and p-0.5 t for the La2001b10 solution with Td values ranging from 0.2 to 1.2 reveals an in-phase relationship with obliquity for Td values of 0.2, 0.3, 0.4, 1.0, and 1.1 at 90% confidence level (see Figure 4 and Table 1). A Td value of 0.9 results in a near in-phase relation with obliquity. Correlation between LCI and p-0.5 t is significant at $>$99.9% level for all correlations. The highest correlation is observed for a Td of 1.2, but also Td values of 0.3–0.5, 0.9,1.0, and 1.1 produce high correlation coefficients statistically indistinguishable at the 90% confidence level. High correlation coefficients and relatively consistent obliquity phases for Td values of 0.3–0.5 originate from a tuning shifted by one precession cycle.

5. Discussion

5.1. Results of This Study

The La2004$_{(1,1)}$ solution gives a good and highly significant fit (confidence level $>$ 99.9 for all correlations made here) with the proxy color records for both intervals studied in the Monte dei Corvi section. For the younger interval (9–9.6 Ma), a Td value of 1 produces the highest correlation and a Td close to 1 (~0.95–1.05) is most likely when the information about the fit is combined with that of the calculated obliquity phase (see Figure 3). For the older interval (11.5–12.1 Ma), solutions with slightly higher Td values (1.1 and 1.2) provide the highest correlation coefficients, although this is within uncertainty of the fit for the solution with the present-day Td value of 1 (Figure 4). For this interval, solutions are in best agreement with the obliquity phase of proxy data for Td values between ~1 and ~1.1 but also 0.3 and 0.4. The fact that Td values around 1 (i.e., 0.95–1.15) give most consistent results for both investigated time intervals makes this most likely when assuming no major change in Td (and/or dE) over this time interval. However, a substantial change in Td and/or dE between 9 and 12 Ma due to a shift in global tidal patterns or topography may lead to different interpretations. Also, other Td values, as shown for lower values ~0.3, may be expected to lead to good results for one of the discussed intervals, but only one Td option is expected to show good matches for both discussed intervals. In this case this is a Td of ~1. Therefore, a maximum range from 0.95 to 1.15 is suggested for Td in the 11.5–12.1 Ma interval.

10.1002/2014PA002615

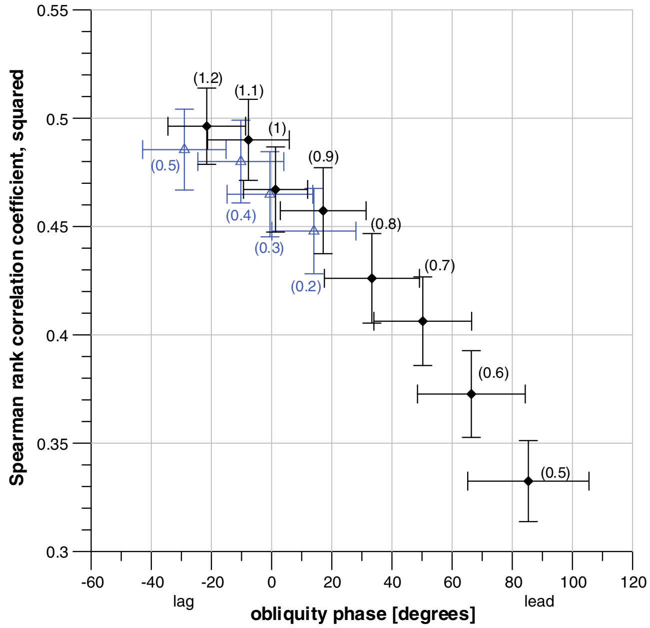

Figure 4. Plot of the squared Spearman rank correlation coefficient (ordinate) versus the obliquity phase (abscissa) of all investigated tunings for the interval from 11.5 to 12.1 Ma. The Td value used for every data point is included. For low Td values (0.2–0.5), the tuning was shifted by one precession cycle; for Td = 0.5, the result of two tuning options is included. Results using a tuning deviating from the tuning used for Td = 0.6 are plotted in blue triangles. The adjustment of the tuning was necessary to achieve a good fit between data and orbital solution.

5.2. Comparison of Results

Our statistical results are in good agreement with the suggestion of *Hüsing et al*. [2007] based on their visual comparison of the cycle patterns. *Hüsing et al*. [2007] investigated the next older 405 kyr maximum in the long-term 2.4 Myr eccentricity minimum from ~12.1 to 12.5 Ma in the Monte dei Corvi section, which was not included in the present study. Accordingly, they found that for this interval, the $La2004_{(1,1.2)}$ solution gives the best fit with the visual characteristics of the lithology (their Figure 8), while the $La2004_{(1,1)}$ solution gives no convincing match. This could indicate that the astronomical solution may indeed require an adjustment of Td to slightly larger than its present-day value to remain in agreement with the proxy data of this older interval. However, statistical analysis of high-resolution proxy data is required for such a statement.

A slightly higher than present Td value for the investigated Miocene time interval is in agreement with the results of *Pälike and Shackleton* [2000] from the equatorial Atlantic Ceara Rise (ODP Leg 154), who suggested an increase of Td over the last 11.5 Ma. However, it is not possible to directly compare our results with those of *Pälike and Shackleton* [2000] and *Lourens et al*. [2001], because they compared their proxy data with the La93 [*Laskar et al*., 1993] solution, which shows different precession-obliquity interference patterns at least for the time interval from 11 to 13 Ma (supporting information Figure S1). This pattern requires a different phasing of both precession and obliquity, which would influence any Td and/or dE values determined relative to the solution using the present-day values. A direct comparison with the study of *Pälike and Shackleton* [2000] is further complicated by the fact that they changed both Td and dE values, while we only considered a change in Td. In addition, the 9–9.6 and 11.5–12.1 Ma intervals were not investigated separately by *Pälike and Shackleton* [2000]. Moreover, the splice, and hence tuning, used by *Pälike and Shackleton* [2000] required partial revision, in particular for the interval between ~10 and 11.5 Ma [*Zeeden et al*., 2013]. Finally, the assumption of a direct response to both precession and obliquity is better substantiated for the Mediterranean than for Ceara Rise.

An average Td value of ≥1 differs considerably from the average Td value of 0.5 inferred by *Lourens et al*. [2001] for the past 3 Ma. The relatively small Td value of 0.5 for the past 3 Ma is, however, statistically hardly distinguishable from the present-day value, since the precession and obliquity periods are quite similar to modern estimates, making it more difficult to discern deviations from present. In addition, the proposed 0.5 Td value could actually be related to major changes in dE associated with the Northern Hemisphere glaciations [e.g., *Laskar et al*., 1993; *Mitrovica et al*., 1994; *Morrow et al*., 2012, and references therein].

5.3. Conceptional Restrictions

Discussed results are based on collected data and their interpretation applying a number of assumptions. We assume an in-phase relation between the lithology-bound color reflectance data and insolation forcing. The most recent sapropel, S1, and the correlative summer insolation maximum are offset by ~2.65 kyr (e.g., *De Lange et al*. [2008] date the S1 between 10.8 and 6.1 ka B.P., while the Northern Hemisphere summer insolation maximum is at 11.1 ka). This ~3 kyr lag was initially assumed for all older sapropels [*Hilgen*, 1991;

L. Lourens et al., 1996], since simple energy balance model simulations confirmed the existence of such a lag [e.g., *Short and Mengel*, 1986]. *Ziegler et al.* [2010] argued, however, that this lag, which is also found in other sapropels of late Pleistocene age, could be related to the occurrence of cold events (i.e., Heinrich events) in the North Atlantic, delaying the direct response of the African monsoon to insolation forcing. Because no such events are known from the generally warmer Miocene climates, Miocene sapropels are assumed to respond directly to insolation forcing, as also suggested by transient modeling experiments, which did not reveal a time lag between North African monsoon precipitation and orbital forcing in model runs without large ice sheets [*Weber and Tuenter*, 2011].

Before interpretations are made in this study, records are tuned to the La2001b10 solution with a specific Td value. Tuning is straightforward when the pattern of the solution and geological pattern match well. However, when these patterns do not match well, and the obliquity phase of record and solution are inconsistent, different tuning options arise (see, e.g., the tuning of the 11.5–12.1 Ma interval for Td ≤ 0.5). For the tunings, we used both prominent cycle pattern and constraints given by sedimentation rates (tie points are displayed in the supporting information Tables S1 and S2).

More specifically, the pattern of the sapropels and the LCI in the older (11.5–12.1 Ma) interval is unusual in so far that the two oldest sapropels (numbers 58 and 59, see Figure 2) are surprisingly distinct. This may point to a nonlinear response to eccentricity and/or obliquity and precession (as discussed by, e.g., *Fischer et al.* [1991]), because strongest sapropels are expected in the middle of a ~405 kyr eccentricity maximum and not at the beginning. However, this does not affect the outcome of our comparison as cross-spectral analysis between orbital solution and proxy data excluding the older 5 m of the record yields very similar results for a limited number of solutions tested.

No claim can be made here about values for Td and dE; only their sum effect can be investigated, limiting geophysical interpretations regarding Td and/or dE. Interpreting our findings as dE, and using the relationship between phase difference and dE as presented by *Lourens et al.* [2001], the uncertainty in the obliquity phase as determined in this study may explain a change in average dE of ~0.001 and ~0.003 over the last ~9 or 12 Ma, respectively. These results and their limit in precision allow most of the models discussed by *Morrow et al.* [2012] to be consistent with our findings. However, *Laskar et al.* [2004] suggested that mantle convection and tidal dissipation may have similar opposite effects for the precession constant. Geophysical models incorporating both mantle convection and tidal dissipation may therefore be useful to solve the discrepancy between some geophysical models and geological observations. We concur with *Morrow et al.* [2012] that long and continuous records are required to solve the potential discrepancy between observation and model results.

5.4. Implications for the Astronomically Tuned Miocene Time Scale

The standard Astronomically Tuned Neogene Time Scale [*Hilgen et al.*, 2012 in *Gradstein et al.*, 2012] is underlain by the tuning of the Monte dei Corvi section for the interval between 8.7 and 14.9 Ma, including the two intervals studied here. Because Td (and also dE) affects the precession and obliquity frequency, a specific change in average Td may be directly translated into a change in timing of specific cycles at any given time. Uncertainties in the precession cycle ages resulting from the uncertainty in Td values (see section 5.1) are ±0.8 kyr for the younger interval (9–9.6 Ma) and +4/−1 (where + represents younger times) kyr for the older interval (11.5–12.1 Ma). These uncertainties rely on the correct tuning of the record but then may be considered full uncertainties and not the mean of Gaussian or skewed distributions with associated probabilities exceeding confidence limits. Confidence in the obliquity phase is similar to that of the precession phase, but result in twice as much temporal uncertainty. For time intervals younger than 9 Ma, the presented data sets do not allow specific conclusions to be made on the accuracy of the time scale; also for intervals older than 12 Ma, no suggestion about the age uncertainty for precession and obliquity can be made.

Summarizing, these new results combined with those of previous studies suggest that potential changes in the astronomically tuned time scale, resulting from the uncertainty in Td and dE values, are small over the last 12 Ma.

5.5. Consequences for Integrated Stratigraphy and Time Scales

Obtaining realistic uncertainties for astronomically tuned time scales is difficult but is important especially for intercalibration with other dating techniques. Attempts for obtaining realistic error estimates have been made through intercalibration with $^{40}Ar/^{39}Ar$ dating [e.g., *Kuiper*, 2003; *Kuiper et al.*, 2008; *Rivera et al.*, 2011].

The intercalibration between astronomical and $^{40}Ar/^{39}Ar$ dating was achieved by dating single crystal sanidines extracted from ash layers intercalated in an astronomically tuned section to cross-calibrate the most widely used $^{40}Ar/^{39}Ar$ monitor [*Kuiper et al.*, 2008; *Rivera et al.*, 2011]. If one assumes similar uncertainties in the time scale for the interval younger than 9.0 Ma as for ~9 Ma, the maximum change in the astronomical age of the ash layers was sufficiently incorporated in uncertainties of ash layer ages by *Kuiper et al.* [2008] and *Rivera et al.* [2011]. Discrepancies of reported ages for $^{40}Ar/^{39}Ar$ dating standards relative to the ones intercalibrated [*Channell et al.*, 2010; *Renne et al.*, 2010] with astronomical time scales [*Kuiper et al.*, 2008; *Rivera et al.*, 2011] can probably not be attributed to the effect of Td and dE.

The estimation of uncertainties associated with magnetic reversal boundaries is complex, as several processes have to be considered. The time it takes for the field to reverse is estimated at 7 kyr but varies with latitude [*Clement*, 2004]. Uncertainties related to delayed lock-in of natural remanent magnetization (NRM) are very difficult to estimate as this can occur early, but also late diagenetic, well after the deposition and deep within the sediment. Delayed NRM acquisition may make a reversal appear older; up to several (hundreds of) thousands of years. In the Monte dei Corvi/La Vedova composite section, the uncertainties of reversal ages are given entirely based on the interpolation between two reliable samples, one having reverse and the other having normal polarity [*Hüsing et al.*, 2007, 2010; *Mourik et al.*, 2010]. The uncertainties of some reversal ages older than 11.5 Ma have stratigraphic uncertainties smaller than the +4 kyr Td uncertainty. As chron boundary ages are determined from orbitally tuned sections and cores for most of the Neogene [*Hilgen et al.*, 2012], the age uncertainty in the tuning and stratigraphic position may be seen as minimum uncertainties. The same holds for biostratigraphic datums.

5.6. Consequences for Determining Phase Relations in the Miocene

Uncertainties in the precession phase of the La2004 solution are ±0.8 kyr (9–9.6 Ma) and +4/−1 kyr (11.5–12.1 Ma); the obliquity phase is accurate to ±1.6 kyr for the interval from 9 to 9.6 Ma, and accurate to +8/−2 kyr only (where + represents younger times) for the 11.5–12.3 Ma interval. The precession phase inaccuracy is probably unproblematic for most records tuned mainly to eccentricity maxima, as a change in Td basically shifts precession during eccentricity maxima. However, during eccentricity minima, the intricate pattern of the orbital solution may change substantially due to also precession frequency modulation by eccentricity [e.g., *Hinnov*, 2000; *Huybers and Aharonson*, 2010]. Tuning to a wrong orbital target results in less precision of determined relative phases.

5.7. Outlook

Higher-quality data, such as the Ti/Al ratio used by *Lourens et al.* [2001], showing a near linear response in both directions of the insolation forcing, may improve our results and thus allow for a more precise quantification of Td and/or dE values and time scales. This is fundamental for paleoclimate studies focusing on phase relations between insolation forcing, climate response, and the registration in the sedimentary archives. To further constrain Td and/or dE, it is proposed to consistently obtain values for (the maximal discrepancy of) the obliquity phase from proxy data with well-known climate response over the last 12 Ma [*Morrow et al.*, 2012]; this approach can then be extended to older time intervals than covered by this study. Replicate studies would be beneficial to validate or challenge the findings of *L. J. Lourens et al.* [1996], *Lourens et al.* [2001], *Pälike and Shackleton* [2000], and this study. Acquiring data from the paleo-Mediterranean may be a favorable option due to the relatively well-known climatic response and origin of sapropels, partly as a consequence of modeling studies that have been carried out [*Tuenter et al.*, 2007; *Weber and Tuenter*, 2011]. More sapropel records of Miocene, Pliocene, and Pleistocene age should thus be investigated in high resolution in order to determine the climate response to insolation forcing through time, and to investigate the effect of Td and/or dE.

6. Conclusions

For the two Miocene intervals studied (~9–9.6 and 11.5–12.1 Ma), the intricate cycle patterns in quantitative proxy records of the Monte dei Corvi record cannot be distinguished statistically from the $La2004_{(1,1)}$ solution, although small discrepancies are found. The data presented limit the (un)certainty of astronomically tuned precession ages to ±0.8 kyr for the ~9–9.6 Ma interval and to +4/−1 kyr (where + represents younger times) for the ~11.5–12.1 Ma interval. These (un)certainties need to be incorporated into Neogene tuned time scales and provide minimum uncertainties for ages of biostratigraphic events and magnetic reversal and stage boundaries. Uncertainties on the precession and obliquity phases limit the determination of precise phase relations between orbital targets and climate proxy data. However, the approach presented in this paper for the first time facilitates the quantitative estimation of uncertainties in Miocene tuned time scales and in the obliquity phase of proxy data. As such, it contributes to determining the accuracy of phase relations between insolation forcing and climate response during the Miocene.

Acknowledgments
This work benefited greatly from thorough and constructive reviews by Stephen Meyers and an anonymous reviewer, whom we would like to thank here. Janja de Jonge, Joyce Bosmans, and Tim van Peer are thanked for their help during field work. Hemmo Abels is thanked for numerous enlightening discussions. This is a contribution made within the GTSnext project (www.gtsnext.eu). The research leading to these results has received funding from the (European Community's) Seventh Framework Programme (FP7/2007-2013) under grant agreement (215458).

References

Blackman, R. B., and J. W. Tukey (1958), *The Measurement of Power Spectra From the Point of View of Communication Engineering*, Dover Publications, New York.

Channell, J. E. T., D. A. Hodell, B. S. Singer, and C. Xuan (2010), Reconciling astrochronological and ^{40}Ar/^{39}Ar ages for the Matuyama-Brunhes boundary and late Matuyama Chron, *Geochem. Geophys. Geosyst. 11*, Q0AA12, doi:10.1029/2010GC003203.

Cleaveland, L., J. Jensen, S. Goese, D. Bice, and A. Montanari (2002), Cyclostratigraphic analysis of pelagic carbonates at Monte dei Corvi (Ancona, Italy) and astronomical correlation of the Serravallian-Tortonian boundary, *Geology*, *30*(10), 931–934, doi:10.1130/0091-7613(2002)030<0931:CAOPCA>2.0.CO;2.

Clement, B. M. (2004), Dependence of the duration of geomagnetic polarity reversals on site latitude, *Nature*, *428*(6983), 637–640, doi:10.1038/nature02459.

De Lange, G., J. Thomson, A. Reitz, C. Slomp, M. Principato, E. Erba, and C. Corselli (2008), Synchronous basin-wide formation and redox-controlled preservation of a Mediterranean sapropel, *Nat. Geosci.*, *1*(9), 606–610, doi:10.1038/ngeo283.

Ebisuzaki, W. (1997), A method to estimate the statistical significance of a correlation when the data are serially correlated, *J. Clim.*, *10*(9), 2147–2153, doi:10.1175/1520-0442(1997)010<2147:AMTETS>2.0.CO;2.

Efron, B., and G. Gong (1983), A leisurely look at the bootstrap, the jackknife, and cross-validation, *Am. Stat.*, *37*(1), 36–48, doi:10.1080/00031305.1983.10483087.

Fischer, A. G., T. D. Herbert, G. Napoleone, I. P. Silva, and M. Ripepe (1991), Albian pelagic rhythms (Piobbico core), *J. Sediment. Petrol.*, *61*(7), 1164–1172.

Gradstein, F., J. Ogg, M. Schmitz, and G. Ogg (Eds) (2012), *The Geologic Time Scale 2012*, Elsevier, Amsterdam.

Hilgen, F. (1991), Astronomical calibration of Gauss to Matuyama sapropels in the Mediterranean and implication for the geomagnetic polarity time scale, *Earth Planet. Sci. Lett.*, *104*(2-4), 226–244, doi:10.1016/0012-821X(91)90206-W.

Hilgen, F., H. Abdul Aziz, W. Krijgsman, I. Raffi, and E. Turco (2003), Integrated stratigraphy and astronomical tuning of the Serravallian and lower Tortonian at Monte dei Corvi (Middle-Upper Miocene, northern Italy), Palaeogeography, Palaeoclimatology, *Palaeoecology*, *199*(3-4), 229–264, doi:10.1016/S0031-0182(03)00505-4.

Hilgen, F., H. Aziz, D. Bice, S. Iaccarino, W. Krijgsman, K. Kuiper, A. Montanari, I. Raffi, E. Turco, and W. Zachariasse (2005), The global boundary stratotype section and point (GSSP) of the Tortonian stage (Upper Miocene) at Monte Dei Corvi, *Episodes*, *28*(1), 6–17.

Hilgen, F., L. Lourens, and J. Van Dam (2012), The Neogene Period, in *The Geologic Time Scale 2012*, edited by F. Gradstein et al., pp. 923–978, Elsevier, Amsterdam.

Hinnov, L. (2000), New perspectives on orbitally forced stratigraphy, *Annu. Rev. Earth Planet. Sci.*, *28*(1), 419–475, doi:10.1146/annurev.earth.28.1.419.

Hüsing, S., F. Hilgen, H. Abdul Aziz, and W. Krijgsman (2007), Completing the Neogene geological time scale between 8.5 and 12.5 Ma, *Earth Planet. Sci. Lett.*, *253*(3-4), 340–358, doi:10.1016/j.epsl.2006.10.036.

Hüsing, S., K. Kuiper, W. Link, F. Hilgen, and W. Krijgsman (2009a), The upper Tortonian-lower Messinian at Monte dei Corvi (Northern Apennines, Italy): Completing a Mediterranean reference section for the Tortonian Stage, *Earth Planet. Sci. Lett.*, *282*(1-4), 140–157, doi:10.1016/j.epsl.2009.03.010.

Hüsing, S., M. Dekkers, C. Franke, and W. Krijgsman (2009b), The Tortonian reference section at Monte dei Corvi (Italy): Evidence for early remanence acquisition in greigite-bearing sediments, *Geophys. J. Int.*, *179*, 125–143, doi:10.1111/j.1365-246X.2009.04301.x.

Hüsing, S., A. Cascella, F. Hilgen, W. Krijgsman, K. Kuiper, E. Turco, and D. Wilson (2010), Astrochronology of the Mediterranean Langhian between 15.29 and 14.17 Ma, *Earth Planet. Sci. Lett.*, *290*(3-4), 254–269, doi:10.1016/j.epsl.2009.12.002.

Huybers, P., and O. Aharonson (2010), Orbital tuning, eccentricity, and the frequency modulation of climatic precession, *Paleoceanography*, *25*, PA4228, doi:10.1029/2010PA001952.

Kuiper K. (2003), Direct intercalibration of radio-isotopic and astronomical time in the Mediterranean Neogene, Faculteit Aardwetenschappen Universiteit Utrecht.

Kuiper, K., A. Deino, F. Hilgen, W. Krijgsman, P. Renne, and J. Wijbrans (2008), Synchronizing rock clocks of Earth history, *Science*, *320*(5875), 500, doi:10.1126/science.1154339.

Laskar, J. (1990), The chaotic motion of the solar system: A numerical estimate of the size of the chaotic zones, *Icarus*, *88*(2), 266–291, doi:10.1016/0019-1035(90)90084-M.

Laskar, J. (2001), Astronomical solutions for paleoclimate studies, AGU Fall Meeting 2001 Abstracts U11A-01.

Laskar, J., F. Joutel, and F. Boudin (1993), Orbital, precessional, and insolation quantities for the Earth from -20 Myr to +10 Myr, *Astron. Astrophys.*, *270*(1-2), 522–533.

Laskar, J., P. Robutel, F. Joutel, M. Gastineau, A. Correia, and B. Levrard (2004), A long-term numerical solution for the insolation quantities of the Earth, *Astron. Astrophys.*, *428*(1), 261–285, doi:10.1051/0004-6361:20041335.

Lourens, L., F. Hilgen, I. Raffi, and C. Vergnaud-Grazzini (1996), Early Pleistocene chronology of the vrica section (Calabria, Italy), *Paleoceanography*, *11*(6), 797–812, doi:10.1029/96PA02691.

Lourens, L. J., A. Antonarako, F. J. Hilgen, A. A. M. Van Hoof, C. Vergnaud-Grazzini, and W. J. Zachariasse (1996), Evaluation of the Plio-Pleistocene astronomical timescale, *Paleoceanography*, *11*, 391–413, doi:10.1029/96PA01125.

Lourens, L., R. Wehausen, and H. Brumsack (2001), Geological constraints on tidal dissipation and dynamical ellipticity of the Earth over the past three million years, *Nature*, *409*(6823), 1029–1033, doi:10.1038/35059062.

Lourens, L., F. Hilgen, N. Shackleton, J. Laskar, and D. Wilson (2004), The Neogene Period, in *A Geologic Time Scale*, edited by F. Gradstein, J. Ogg, and A. Smith, pp. 409–440, Cambridge Univ. Press, Cambridge.

Mader, D., A. Montanari, J. Gattacceca, C. Koeberl, R. Handler, and R. Coccioni (2001), 40Ar/39Ar dating of a Langhian biotite-rich clay layer in the pelagic sequence of the Conero Riviera, Ancona, Italy, *Earth Planet. Sci. Lett.*, *194*(1-2), 111–126, doi:10.1016/S0012-821X(01)00544-1.

Mader, D., L. Cleaveland, D. Bice, A. Montanari, and C. Koeberl (2004), High-resolution cyclostratigraphic analysis of multiple climate proxies from a short Langhian pelagic succession in the Conero Riviera, Ancona (Italy), *Palaeogeogr. Palaeoclimatol. Palaeoecol.*, *211*(3-4), 325–344, doi:10.1016/j.palaeo.2004.06.001.

Meyers, S. R. (2014), Astro: An R Package for Astrochronology (Version 0.3).

Mitrovica, J. X., R. Pan, and A. M. Forte (1994), Late Pleistocene and Holocene ice mass fluctuations and the Earth's precession constant, *Earth Planet. Sci. Lett.*, *128*, 489–500.

Montanari, A., B. Beaudoin, L. Chan, R. Coccioni, A. Deino, D. DePaolo, L. Emmanuel, E. Fornaciari, M. Kruge, and M. Mozzato (1997), Integrated stratigraphy of the middle to upper Miocene pelagic sequence of the Conero Riviera (Ancona, Italy), *Miocene Integr. Stratigr.*, *15*, 409–450.

Morrow, E., J. Mitrovica, A. Forte, P. Glišović, and P. Huybers (2012), An enigma in estimates of the Earth's dynamic ellipticity, *Geophys. J. Int.*, *191*(3), 1129–1134, doi:10.1111/j.1365-246X.2012.05703.x.

Mourik, A., J. Bijkerk, A. Cascella, S. Hüsing, F. Hilgen, L. Lourens, and E. Turco (2010), Astronomical tuning of the La Vedova High Cliff section (Ancona, Italy) - Implications of the Middle Miocene Climate Transition for Mediterranean sapropel formation, *Earth Planet. Sci. Lett.*, *297*, 249–261, doi:10.1016/j.epsl.2010.06.026.

Paillard, D., L. Labeyrie, and P. Yiou (1996), Macintosh program performs time-series analysis, *Eos Trans.*, *77*(39), 379, doi:10.1029/96EO00259.

Pälike, H., and N. Shackleton (2000), Constraints on astronomical parameters from the geological record for the last 25 Myr, *Earth Planet. Sci. Lett.*, *182*(1), 1–14, doi:10.1016/S0012-821X(00)00229-6.

Pearson, K. (1896), Mathematical contributions to the theory of evolution. III. Regression, heredity, and panmixia, *Philos. Trans. R. Soc. London. Ser. A Containing Pap. Math. Phys. Charact.*, *187*, 253–318, doi:10.1098/rsta.1896.0007.

Quinn, T. R., S. Tremaine, and M. Duncan (1991), A 3 million year integration of the Earth's orbit, *Astron. J.*, *101*(6), 2287–2305.

Renne, P. R., R. Mundil, G. Balco, K. Min, and K. R. Ludwig (2010), Joint determination of ^{40}K decay constants and ^{40}Ar*/^{40}K for the Fish Canyon sanidine standard, and improved accuracy for ^{40}Ar/^{39}Ar geochronology, *Geochim. Cosmochim. Acta*, *74*, 5349–5367, doi:10.1016/j.gca.2010.06.017.

Rivera, T. A., M. Storey, C. Zeeden, F. J. Hilgen, and K. Kuiper (2011), A refined astronomically calibrated 40Ar/39Ar age for Fish Canyon sanidine, *Earth Planet. Sci. Lett.*, *311*(3-4), 420–426, doi:10.1016/j.epsl.2011.09.017.

Shackleton, N. and S. Crowhurst (1997), Sediment fluxes based on an orbitally tuned time scale 5 Ma to 14 Ma, Site 926, in *Proc. ODP, Sci. Results*, vol. 154, edited by N. Shackleton et al., pp. 69–82, Ocean Drilling Program, College Station, TX, doi:10.2973/odp.proc.sr.154.102.

Short, D., and J. Mengel (1986), Tropical climatic phase lags and Earth's precession cycle, *Nature*, *323*, 48–50, doi:10.1038/323048a0.

Spearman, C. (1904), The proof and measurement of association between two things, *Am. J. Psychol.*, *15*(1), 72–101.

Tuenter, E., S. Weber, F. Hilgen, and L. Lourens (2003), The response of the African summer monsoon to remote and local forcing due to precession and obliquity, *Global Planet. Change*, *36*(4), 219–235, doi:10.1016/S0921-8181(02)00196-0.

Tuenter, E., S. Weber, F. Hilgen, and L. Lourens (2007), Simulating sub-Milankovitch climate variations associated with vegetation dynamics, *Clim Past*, *3*(1), 169–180, doi:10.5194/cp-3-169-2007.

Turco, E., A. Cascella, R. Gennari, F. Hilgen, S. Iaccarino, and L. Sagnotti (2011), Integrated stratigraphy of the La Vedova section (Conero Riviera, Italy) and implications for the Burdigalian/Langhian boundary, *Stratigraphy*, *2-3*(8), 89–110.

Weber, S., and E. Tuenter (2011), The impact of varying ice sheets and greenhouse gases on the intensity and timing of boreal summer monsoons, *Quat. Sci. Rev.*, *30*(3), 469–479, doi:10.1016/j.quascirev.2010.12.009.

Zeeden, C., F. Hilgen, T. Westerhold, L. Lourens, U. Röhl, and T. Bickert (2013), Revised Miocene splice, astronomical tuning and calcareous plankton biochronology of ODP Site 926 between 5 and 14.4 Ma, *Palaeogeogr. Palaeoclimatol. Palaeoecol.*, *369*, 430–451, doi:10.1016/j.palaeo.2012.11.009.

Ziegler, M., E. Tuenter, and L. Lourens (2010), The precession phase of the boreal summer monsoon as viewed from the eastern Mediterranean (ODP Site 968), *Quat. Sci. Rev.*, *29*(11), 1481–1490, doi:10.1016/j.quascirev.2010.03.011.